Draft. The final, published version of this paper can be found in:
Magazine of Concrete Research vol. 55, No. 3, June 2003. pp. 249-256

A Maturity Approach to the Rate of Heat Evolution in Concrete

Y. Ballim and PC Graham
School of Civil and Environmental Engineering, University of the Witwatersrand
Private Bag 3, WITS, 2050, Johannesburg, South Africa
(e-mail: ballim@civil.wits.ac.za)

Abstract
This paper discusses the use of the concept of maturity as a means of combining the effects of time and temperature in describing the rate of heat evolution from hydrating cement in concrete. The proposed maturity approach allows the rate of heat evolution determined from an adiabatic test to be expressed in a form which is independent of the starting temperature of the test. This relationship can then be directly used in a time-temperature prediction model which requires a solution of the Fourier equation for heat flow.

The results of an experimental study aimed at assessing the suitability of both the Arrhenius and Nurse-Saul maturity relationships are also presented. Three adiabatic calorimeter tests were conducted on each of two concrete mixtures but starting at different temperatures. The results confirm the suitability of this approach and indicate that the Arrhenius maturity relationship is the more suitable in this application.

Keywords: Cement; concrete; hydration; heat; maturity; adiabatic calorimetry; modelling.

Introduction

Early-age cracking as a result of temperature induced stresses can be a serious problem in mass concrete structures or in concrete structural elements in which a high cement content concrete is used. These stresses are induced by temperature differences in the concrete as a result of the heat liberated by hydrating cement. A strategy that is aimed at controlling or limiting such cracking must include a reliable determination of the space-time distribution of temperature throughout the concrete element under consideration.

The distribution of temperature across the concrete section is determined by solution of the Fourier equation which, in its three-dimensional and transient form for concrete, is given as[1]:

$$\rho . C_p . \frac{\partial T}{\partial t} = k\left(\frac{\partial^2 T}{\partial x^2} + \frac{\partial^2 T}{\partial y^2} + \frac{\partial^2 T}{\partial z^2} \right) + \dot{q}_t \qquad (1)$$

where: Δ = density of the concrete; C_p = specific heat capacity of the concrete; T = temperature t = time; k = thermal conductivity of the concrete; x, y, z are the coordinates at a particular point in the structure, and $\dot{q}_t$ = rate of heat evolution from the hydrating cement.

The hydration of cement is an exothermic reaction which, for a portland cement under normal environmental conditions, produces approximately 350 kJ/kg of heat after seven days of hydration[1]. In Equation 1, this is reflected in the heat generation rate term ($\dot{q}_t$), which is time based and usually has units of power per unit volume (J/s.m^3 or W/m^3). At normal hydration temperatures, $\dot{q}_t$ varies with time in a series of distinct phases[2,3]:

Phase 1: Within the first few minutes after water is added to the cement, a brief but rapid rate of heat release occurs as the early hydration of the aluminate phases occurs. The effect of gypsum in limiting this reaction then becomes manifest and the rate of heat evolution drops rapidly and becomes dormant for a period of approximately two hours after mixing.

Phase 2: After initial setting of the cement, the rate of heat evolution rises sharply as the (mainly) C_3S phases are hydrated. This process continues until a peak heat rate is achieved at 6 to 8 hours after mixing.
Phase 3: After this peak is reached, the heat rate drops rapidly until approximately 20 hours after mixing. This occurs as the amount of C_3S available for hydration decreases, the accessibility of such unhydrated C_3S to water is progressively reduced and the hydration of C_2S, with a lower rate of heat output, starts to become significant in the process. Hereafter, the heat rate drops steadily as hydration proceeds so that, by seven days after mixing, the rate of heat evolution under adiabatic conditions is less than 0.2 W/kg of cement.

For the purposes of temperature modelling in large concrete elements at early ages, the heat evolved during the Phase 1 reactions are usually neglected as it is assumed that:

- these reactions take place some time before the concrete is cast into the formwork; and
- the amount of heat evolved during this phase is small and has the effect of causing only a small change in the placing temperature of the concrete.

A numerical solution of Equation 1 requires an accurate assessment of the rate of heat evolution from the hydrating cement over time if such a solution is to be useful to the design engineer. A number of approaches have been used in the past to provide guidance on the rate of heat evolution for use as input in a numerical temperature modelling exercise. These have taken the form of rough, generalised values of total heat liberated over the early period of hydration for different binder types[4] or cement components[5] , guide equations[6] for the rate of heat evolution in Phases 2 and 3 (as described above) or fairly sophisticated models based on the chemistry and crystallography of the cement[7]. More recently, it has been recognised that a laboratory-based measurement is the more reliable measure of the rate of heat evolution and researchers have used techniques such as isothermal methods[8,9], conduction calorimetry[10,11], adiabatic calorimetry[12,13,14] and semi-adiabatic calorimetry[14].

All these approaches are aimed at developing a single relationship, either mathematical or numerical, which expresses the variation in the rate of heat evolution with time or, in many cases, maturity as a measure of the advance of the hydration process. Such an expression then forms the basis for the term $\dot{q}_t$ in Equation 1. An important problem with this approach is that, in this form, the rate of heat evolution relates to a unique temperature regime and time-temperature history under which the hydration process takes place. In this context, the circular problem presented by hydrating cement is that the hydration process evolves heat which changes the temperature of the environment, thus influencing the rate of hydration and heat evolution. The nature of this problem is recognised by van Breugel[15] and he proposes the use of a "process curve" for the total heat evolved, which deviates from the adiabatic (or semi-adiabatic) curve in response to the temperature regime of the actual structure being modelled, as distinct from the temperature regime of the test.

However, in a real concrete structure under normal construction conditions, the temperature varies at different positions across the structure. This means that, at any time after placing the concrete, different points in the structure will have been subjected to different time-temperature histories and, as a consequence, the extent of hydration and the rate of heat evolution will be different at these different points. This means that a each point in the structure experiences a unique $\dot{q}_t = f(t)$ relationship, in response to the unique time-temperature history at that point. The form of the heat rate input curve in a temperature

prediction model must, therefore, be such that it allows for variations in the time-temperature history at different points in the structure.

This paper proposes a maturity form of the rate of heat evolution relationship in order to normalise the heat rate curve determined from a laboratory-based adiabatic temperature test. The proposed form of the relationship allows a single heat rate relationship to be used as input in a temperature simulation model. Using appropriate maturity parameters, this relationship is then adjusted in response to the different time-temperature histories at different locations in the structure.

In order to assess the suitability of the proposed maturity approach to the development of heat rate over time, samples of two concretes, using two binder types were tested in an adiabatic calorimeter with three different starting temperatures for each concrete. The heat rates were then determined and expressed in terms of maturity. These results were also used to assess the suitability of the Arrhenius and Nurse-Saul maturity relationships in this application.

Determining $\dot{q}_t$ from an adiabatic test

Adiabatic testing is a convenient, reproducible and practical means of determining the amount of heat liberated by hydrating cement. It has the added advantage that the test can be conducted on a sample of the actual concrete used in the structure. The test is usually run over a period of up to seven days, by which time, depending on the accuracy of the temperature measuring instruments, the rate of heat evolution of the concrete is so low that no significant increase in temperature of the sample is noted. The output from the test is a measure of the variation of temperature of the concrete sample with time, or *T(t)*. The total heat per unit mass of binder (q_t) generated at any time (t) during the test can then be determined from:

$$q_t = C_p.(T_t - T_o) \cdot \frac{m_s}{m_c} \qquad (2)$$

where C_p is the specific heat capacity of the concrete, determined as the mass weighted average of the specific heat capacities of the concrete components and is assumed to be constant throughout the test[12]; T_t is the temperature of the concrete sample at time t during the adiabatic test and T_o is the sample temperature at the beginning of the test; m_s is the mass of the concrete test sample and m_c is the mass of binder in the sample.

The rate of heat evolution is determined by differentiating Equation 2, so that:

$$\dot{q}_t = \frac{dq_t}{dt} \qquad (3)$$

This then gives a relationship between the rate of heat evolution and time for the adiabatic test. In order to account for time-temperature histories in the actual structure, which will be different from the adiabatic test conditions, the time component of this relationship is converted to maturity in order to account for the combined effect of time and temperature on the extent and rate of hydration[6,15]. Maturity (M) is here defined as:

$$M = \int_0^t f(T).dt \qquad (4)$$

The Nurse-Saul and Arrhenius expressions[16] (discussed later) are most commonly used as the temperature functions (*f(T)*) in Equation 4.

This process results in a relationship between the rate of heat evolution from the concrete and the maturity of the concrete. As an example of this form of the relationship, Wang and Dilger[6] propose the following equation for determining the rate of heat evolution (in W/kg of cement) to be used in Equation 1:

$$\dot{q}_t = 0.5 + 0.54 M^{0.5} \quad for\ M \le 10\,hours$$
$$\dot{q}_t = 2.2 \exp[-0.0286(M - 10)] \quad for\ M \ge 10\,hours \tag{5}$$

where M is the maturity of the concrete relative to that of concrete cured at 20 ^{o}C.

An important weakness with this approach to determining the heat input curve for Equation 1 is that it ignores the temperature at which the adiabatic test was conducted. Equation 2 is concerned only with the difference in temperature and not the absolute temperature at which the test was commenced. The starting temperature of the test will have a significant influence on the rate of hydration and Equation 5 is clearly not able to account for this phenomenon. In fact, the upper limit of 2.2 W/kg for the rate of heat evolution which is set by Equation 5 must be considered as arbitrary since the magnitude and time of occurrence of the maximum hydration rate will depend on the absolute temperature conditions of the hydration process.

A further criticism of rate of heat evolution functions which are similar to that proposed in Equation 5 is that, if at some stage after placing the concrete, the temperature of the concrete is reduced to –10 ^{o}C (when hydration is deemed to cease[16]), the rate of heat evolution will reduce to zero. However, since the cumulative maturity remains constant, Equation 5 will yield a finite and positive heat rate, despite this reduction in temperature.

In order to address this problem, it is necessary to express the heat evolved as measured in the adiabatic test in terms of the "maturity heat rate" as a function of the cumulative maturity, rather than a time rate. The maturity heat rate ($\dot{q}_M$) is expressed as:

$$\dot{q}_M = \frac{dq_t}{dM} \tag{6}$$

and the time-based heat rate, as required in Equation 1, is then determined using the chain rule as follows:

$$\dot{q}_t = \dot{q}_M \frac{dM}{dt} \tag{7}$$

Hence, in the operation of temperature prediction models for concrete, it is necessary to maintain a measure of both the development and the time based rate of change of maturity at each point under consideration in the concrete element. The form of the heat rate expression as presented in Equations 6 and 7 also address the problem presented above, where the temperature of the concrete is suddenly reduced to –10 ^{o}C. In this case, the time-rate of change of maturity is zero and Equation 7 correctly yields a $\dot{q}_t$ value of zero.

Experimental assessment of the proposed heat rate relationship

Materials and concrete mixtures

In order to assess the suitability of the heat rate expressions as proposed in Equations 6 and 7, adiabatic tests were conducted using two concrete mixtures, each with three different starting temperatures. Table 1 shows the composition of the concretes tested while Table 2 shows the chemical composition of the Portland cement (CEM I) and the ground granulated blast furnace slag (GGBS) as determined from an X-ray fluorescence analysis. The aggregate used

is a clean, washed quartz sand and stone with a chunky to rounded particle shape. The grading of the sand was controlled by recombining the different size fractions in the required proportions for each mixture.

The mixtures were designed to produce lean concretes with a relatively high w/c ratio. This was considered to be typical of mixtures used in mass concrete construction. Furthermore, the mixtures were selected to assess the applicability of the proposed heat rate expressions to concretes with different binder types.

Table 1. Composition of the concrete mixtures used in the adiabatic tests

	MIX A	MIX B
Portland cement (CEM I)	350 kg/m^3	210 kg/m^3
GGBS	-	140 kg/m^3
9.5 mm quartz stone	850 kg/m^3	850 kg/m^3
graded quartz sand	885 kg/m^3	885 kg/m^3
Water	233 L/m^3	233 L/m^3

Table 2. XRF analysis of the cement and GGBS used in the concretes

	Composition (%)	
	Cement	GGBS
CaO	65.52	34.76
SiO_2	21.80	37.18
Fe_2O_3	2.21	0.59
Al_2O_3	4.04	13.35
MgO	1.46	10.98
TiO_2	0.32	0.66
Mn_2O_3	0.15	0.81
K_2O	0.18	0.70
Na_2O	0.00	-
SO_3	2.00	1.03
P_2O_5	0.00	-
Free Lime	0.00	-
LOI	2.30	-
TOTAL	99.98	100.06

Description of the adiabatic calorimeter

A schematic arrangement of the calorimeter used in this investigation is presented in Figure 1. In principle, the test involves placing a one litre sample of concrete in a water bath, such that a stationary pocket of air separates the concrete sample from the water. The signal from a thermal probe placed in the sample is monitored by a desk-top computer and, via an input/output analogue to digital conversion card, the heater in the water bath is turned on and off so as to maintain the water at the same temperature as the concrete. This ensures that there is no exchange of heat between the concrete sample and the surrounding environment. The pocket of air around the sample is important to dampen out any harmonic response between the sample and water temperature as a result of the measurement sensitivity of the thermal probes. The test is usually run over a period of between 5 and 7 days, by which time the rate of heat evolution of the sample is too low to be detected as a temperature difference by the thermal probes – given that the thermal probes are accurate to approximately 0.5 ^{o}C. Further

details of the construction and operation principles of the calorimeter are provided by Gibbon et al[12].

Figure 1: Schematic arrangement of the adiabatic calorimeter

The calorimeter is calibrated via slope and offset calibration parameters built into the operational software. The system is calibrated after every 10 adiabatic tests or when a temperature probe is replaced, to ensure that:

- the difference in temperature readings between the sample and water temperature probes is less than 0.05 ^{o}C over a temperature range of 5 to 65 ^{o}C;
- the difference between the probe temperature readings and that of a calibrating glass thermometer is less than 0.5 ^{o}C over a temperature range of 5 to 65 ^{o}C;
- the measured heat rates on successive tests of the same concrete mixture, using materials from the same batch and under the same starting temperature conditions, do not differ by more than 7% at any time during the test.

Before the adiabatic test was conducted, the temperature in the test room was adjusted to the intended start temperature of the test. The calorimeter and all the components of the concrete were stored in this room for at least 24 hours before commencement of the test. A one litre sample of concrete was used in all the tests and, after assembly of the sample in the calorimeter, measurement of concrete temperature was started within 15 minutes after the water was added to the concrete.

Maturity functions

Both the Arrhenius and the Nurse-Saul maturity functions were assessed for appropriateness in this application. These functions are more often used to predict the hardened properties of concrete such as strength[16,17] and, in this context, Naik[18] has raised questions regarding the accuracy and appropriateness of the Nurse-Saul function, particularly at low temperatures. The functions were used in their relative form with respect to concrete cured at 20 ^{o}C. In this form, the maturity of concrete cured at any temperature is expressed as the equivalent maturity time (t_{20}) of a concrete cured at 20 ^{o}C. If the test concrete is continuously cured at 20 ^{o}C, the maturity time is equal to the clock time.

For the analysis of results from an adiabatic calorimeter test, in which temperature was measured over *n*, unequally spaced time intervals, the functions were used in the following forms:

Arrhenius function:

$$t_{20} = \sum_{i=1}^{i=n} \exp\left[\left(\frac{E}{R}\right)\left(\frac{1}{293} - \frac{1}{273 + 0.5.\left(T_i + T_{i-1}\right)}\right)\right] \cdot \left(t_i - t_{i-1}\right) \quad (8)$$

Nurse-Saul function:

$$t_{20} = \sum_{i=1}^{i=n} \left(\frac{0.5.\left(T_i + T_{i-1}\right) + 10}{30}\right) \cdot \left(t_i - t_{i-1}\right) \quad (9)$$

In Equations 8 and 9, t_{20} is the equivalent maturity time (in hours); E is the activation energy parameter; R is the universal gas constant (8.314 J/mol.^{o}C); T_i is the temperature (^{o}C) at the end of the i^{th} time interval, t_i. The value of E was taken as a constant (= 33.5 kJ/mol) as

suggested by Bamford and Tipper[19]. Broda et al[20] have shown that *E* varies with temperature during hydration but note that the variation is fairly small and that a single value would suffice. In an assessment of blended cements using isothermal calorimetry, Xiong and van Breugel[21] show similar variations in the apparent activation energy with the progress of hydration. However, they also conclude that this variation ".. may be less important in real engineering practice ..".

Results and discussion

By application of Equation 2, the temperatures measured in the adiabatic calorimeter tests were used to determine the heat output for Mixes A and B when tested at different starting temperatures. These results are shown in Fig. 2(a) and 2(b), together with the starting temperatures used for each of the tests.

Fig. 2. Calculated heat output for the three adiabatic tests conducted on each concrete mixture

Fig. 2(a) shows that, for the CEM I concrete, after approximately 60 hours under adiabatic conditions, the sample started at 13 ^{o}C produces more total heat than the samples started at the higher temperatures. This is consistent with earlier experience regarding compressive strength of concretes in that concretes cured at lower initial temperatures show higher strengths at later ages[22]. This is also evident for the GGBS concrete (Fig 2(b)) but only in that, after 50 hours, the sample started at 12 ^{o}C produces more heat than the sample started at 17 ^{o}C. Unlike the CEM I concrete, the low temperature GGBS sample does not produce more heat than the high temperature GGBS sample and this may be a reflection of the improved hydration characteristics of GGBS concretes as the temperature increases[23].

Figure 3 shows the heat curves of Fig. 2 converted to heat rate curves ($\dot{q}_t = f(t)$) using Equation 3. It is clear that this form of the heat rate curve is inappropriate as the input curve for a concrete temperature prediction model since both the magnitude and time distribution of the heat rate depend on the starting temperature of the adiabatic calorimeter test.

Fig. 3. Variation of the time-based heat rates determined from the adiabatic tests

Fig. 4 shows the maturity heat rates plotted against the cumulative maturity of the concretes over the duration of testing. Fig. 4(a) shows the results based on the Arrhenius maturity function (Equation 8) while the Nurse-Saul maturity function (Equation 9) was used to generate the results shown in Fig. 4(b). In both these figures, the maturity heat rate is $\dot{q}_M$ as defined in Equation 6 and is expressed in units of kJ/t_{20} second/kg of cement.

Fig. 4. Heat rates expressed in terms of maturity using the Arrhenius maturity function for the two concretes assessed.

Fig. 4 shows that, when the heat rate is expressed as the Arrhenius maturity heat rate (as defined in Equation 6), with respect to the cumulative Arrhenius maturity, the heat rate curves of Fig. 3 are normalised both in magnitude and maturity distribution. This occurs both for the plain CEM I concrete and for the GGBS blended concrete. The curves for both concretes show a brief spike of heat rate for the tests started at the high temperature. This feature was confirmed on repeat testing and it appears to be a characteristic of the cements and concretes

tested. However, the relatively short duration of this spike probably means that it is not significant for modelling of temperatures in mass concrete structures.

Figure 5 shows the results of the tests on the CEM I concrete expressed in a similar manner as in Fig. 4 but using the Nurse-Saul maturity expression. It is clear that the Nurse-Saul relationship normalises the curves to the extent that the peak heat rates occur at approximately the same maturity time. However, while there is reasonable agreement in the heat rate curves for the tests started at 13 ^{o}C and 21 ^{o}C, the 29 ^{o}C curve is not normalised to the same curve, especially in the range of the peak heat rate. This appears to reinforce Naik's observation[16] that the Nurse-Saul function is reliable only over a limited temperature range. Nevertheless, it appears that, of the two functions assessed, the Arrhenius function is the preferred function for developing a normalised heat rate curve as input into a temperature prediction model based on a solution of Equation 1.

Figure 5: Heat rates of the CEM I concrete expressed in terms of maturity using the Nurse-Saul maturity function

The weakness of approaches such as that proposed in Equations 5 is demonstrated in Fig. 6, where the time-based heat rate ($\dot{q}_t$) for each of the three adiabatic tests conducted on the CEM I concrete is presented as a function of the Arrhenius maturity. This figure clearly shows the dependence of the heat rate on the temperature conditions under which the adiabatic test was conducted. This form of expression of the heat rate is therefore not suitable as input into a temperature prediction model.

Figure 6: Relationship between the time-based heat rate ($\dot{q}_t$) of the CEM I concrete samples and the corresponding Arrhenius maturity.

Using the normalised maturity heat rate curve in a temperature prediction model

Temperature prediction models for concrete are normally finite element or finite difference models which involve a numerical, stepwise solution of Equation 1 and a value of $\dot{q}_t$ is required at each time interval of the analysis. The input curve for this analysis, derived from an adiabatic (or semi-adiabatic) test, should be constructed as a $\dot{q}_M = f(M)$ curve as shown in Fig. 4. In this form, an appropriate and different time-based heat rate curve can be determined for each point in the structure which is subjected to a different time-temperature history. This is achieved by structuring the heat model so as to maintain a continuous calculation of the cumulative maturity as well as the time rate of change of maturity at each location of analysis in the concrete element. At each time interval in the analysis, the maturity heat rate is then determined from the input curve, based on the cumulative maturity at the particular point. The time-based heat rate is then determined by multiplication with the rate of change of maturity, as indicated in Equation 7. As an example of the form in which this calculation should be maintained, Fig. 7 shows the variation of Arrhenius maturity with time for the three adiabatic tests conducted on the CEM I concrete. As a reference, Fig. 7 also shows the maturity development of a concrete continuously cured at 20 ^{o}C, for which the maturity time is equal to the clock time.

Fig. 7. Variation in cumulative maturity of the CEM I concrete in the three adiabatic tests

In a concrete temperature prediction model, maturity curves similar to those shown in Fig. 7 should be developed for each location (or node) of analysis in the actual structure, based on the time-temperature history at that location. In this form, both the maturity (M) and the rate of change of maturity $\left(\frac{dM}{dt}\right)$ can easily be determined at each time-step in the analysis. This will result in a more accurate prediction of the likely temperature profiles in mass concrete structures, allowing engineers and concrete technologists to better manage issues such as:

- selecting appropriate cements and cement blends in order to minimise the temperature development in the structure;
- designing pre-cooling and in situ cooling systems to reduce the maximum temperature in the concrete structure;
- estimating the appropriate time for joint grouting in mass concrete structures.

Conclusions

1. In order to account for variations in the early-age rate of hydration (and, hence, heat evolution) of cement and cement blends as a result of different time-temperature conditions, the rate of heat evolution must be normalised by being expressed as a maturity heat rate in the form $\frac{dq_t}{dM}$. Furthermore, the heat rate input curve for a concrete temperature prediction model involving a solution of the Fourier equation should be expressed as $\frac{dq_t}{dM} = f(M)$, where q_t is the heat produced by hydrating cement (J/kg of cement) and M is the maturity.
2. Numerical temperature prediction models for concrete must be constructed so as to maintain a cumulative calculation of maturity and the rate of change of maturity at each location or node of analysis in the concrete element under consideration.
3. In this context, The Arrhenius maturity function provides a good basis for normalising the heat rate curves and this function should be used in preference to the Nurse-Saul maturity function.
4. The experimental verification presented in this investigation shows that the proposed maturity form of the heat rate curve is appropriate for use with concretes containing CEM I or GGBS blended cements.

References

1. HOLMAN, J. P. *Heat Transfer*, 7th Ed. McGraw Hill Inc. New York, 1990.
2. OLDER, I. Hydration, setting and hardening of Portland cement. *Lea's Chemistry of Cement and Concrete*. 4th Edition, HEWLETT, P. C. (ed.), Arnold, London, 1988, pp. 241-297.
3. TAYLOR, H. F. W. *Cement Chemistry* (2nd Edition) Thomas Telford, London, 1997.
4. ADDIS, BJ (ed.). *Fulton's concrete technology. (6th Revised Edition)*. Portland Cement Institute, Midrand, South Africa. 1986, pg. 709.
5. SCANLON, J. M. and McDONALD, J. E. Thermal properties. *Significance of tests and properties of concrete and concrete-making materials*. KLEIGER, P. and LAMOND, J. F. (eds.), ASTM-STP 169C. American Society for Testing and Materials, Philadelphia, 1994, Chapter 24, pp 229-239.
6. WANG, Ch and DILGER, W.H. Prediction of temperature distribution in hardening concrete. In *Thermal Cracking in Concrete at Early Ages*. SPRINGENSCHMID, R (ed.), E&FN Spon, London, 1994, pp. 21-28

7. MAEKAWA, K, CHAUBE, R and KISHI, T. *Modelling of Concrete Performance – Hydration, Microstructure Formation and Mass Transport*. Routledge, London, 1999.
8. BASSON, G. R. Heat of hydration of Portland cement and of mixtures of Portland cement and milled granulated blastfurnace slag with special reference to the heat development in mortars under adiabatic conditions. *Civil Engineer in South Africa*, 1966, **8**, No. 2, 63-67.
9. LAWRENCE, C. D. Physicochemical and mechanical properties of Portland cements. *Lea's Chemistry of Cement and Concrete.* 4th Edition, HEWLETT, P. C. (ed.), Arnold, London, 1988, pp. 343-419.
10. MONFOE, G. E. and OST, B. An "isothermal" conduction calorimeter for study of the early hydration reactions in Portland cement. *Jnl. of PCA Research and Development Laboratories*, 1966, pp. 13-20.
11. KISHI, T. and MAEKAWA, K. Thermal and mechanical modelling of young concrete based on hydration process of multi-component cement minerals. In *Thermal Cracking in Concrete at Early Ages*. SPRINGENSCHMID, R (ed.), E&FN Spon, London, 1994, pp. 12-18
12. GIBBON, G. J., BALLIM, Y. and GRIEVE, G. R. H. A low-cost, computer-controlled adiabatic calorimeter for determining the heat of hydration of concrete. *ASTM Jnl. of Testing and Evaluation*, 1997, 25, No. 2, pp. 261-266.
13. KOENDERS, E. A. B. and VAN BREUGEL, K. Numerical and experimental adiabatic hydration curve determination. In *Thermal Cracking in Concrete at Early Ages*. SPRINGENSCHMID, R (ed.), E&FN Spon, London, 1994, pp. 3-10
14. MORABITU, P. Methods to determine the heat of hydration of concrete. In *Prevention of Thermal Cracking in Concrete at Early Ages*. SPRINGENSCHMID, R (ed.),RILEM Report 15. Chapter 1. E&FN Spon, London, 1998, pp. 1-25.
15. VAN BREUGEL, K. Prediction of temperature development in hardening concrete. In *Prevention of Thermal Cracking in Concrete at Early Ages*. SPRINGENSCHMID, R (ed.), RILEM Report 15. Chapter 4. E&FN Spon, London, 1998, pp. 51-75.
16. NAIK, TR. Maturity functions for concrete cured during winter conditions. In: *Temperature effects on concrete, ASTM STP 858*. NAIK, TR (ed). American Society for Testing Materials, Philadelphia, 1985. 107-117.
17. MITCHELL, D., KHAN, A. A. and COOK, W. D. Early age properties for thermal and stress analyses during hydration. In Materials Science of Concrete V SKALNY, J and MINDESS, S (eds.) American Ceramic Society, Ohio, 1998, pp. 265-305.
18. NAIK, TR. Maturity of concrete: Its applications and limitations. In Advances in Concrete Technology. MALHOTRA, VM (ed.). Natural Resources Canada, Ottawa, 1994, pp. 339-369.
19. BAMFORD, C. H. and TIPPER, C. F. H. (eds.) *Comprehensive chemical kinetics, Vol. 1: The practice of kinetics*. Elsevier Publishing Company, London, 1969.
20. BRODA, M, WIRQUIN, E and DUTHOIT, B. Conception of an isothermal calorimeter for concrete – Determination of the apparent activation energy. *Materials and Structures*, **35**, Aug. 2002, pp. 389-394.
21. XIONG, X and VAN BREUGEL, K. Isothermal calorimetry study of blended cements and its application in numerical simulations. *Heron*, 46, No. 3, 2001, pp. 151-159.
22. MEHTA, P. K. *Concrete structure, properties and materials.* Prentice Hall, New Jersey, 1986.
23. MORANVILLE-REGOURD, M. Cements made from Blastfurnace Slag. *Lea's Chemistry of Cement and Concrete.* 4th Edition, HEWLETT, P. C. (ed.), Arnold, London, 1988, pp. 633-674.

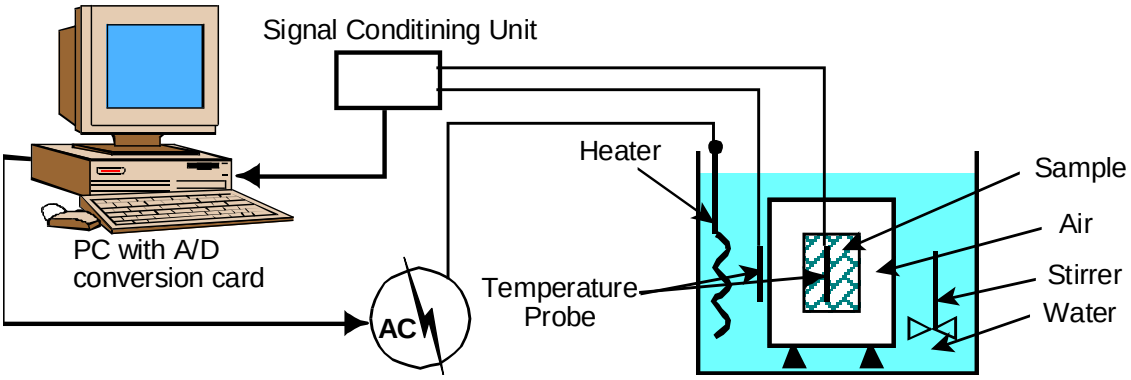

Figure 1: Schematic arrangement of the adiabatic calorimeter

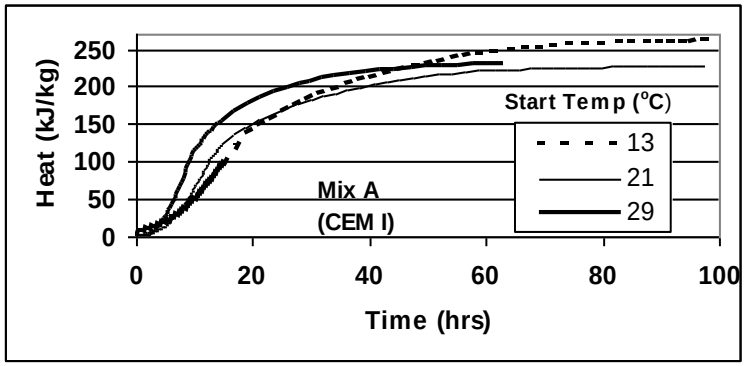

(a)

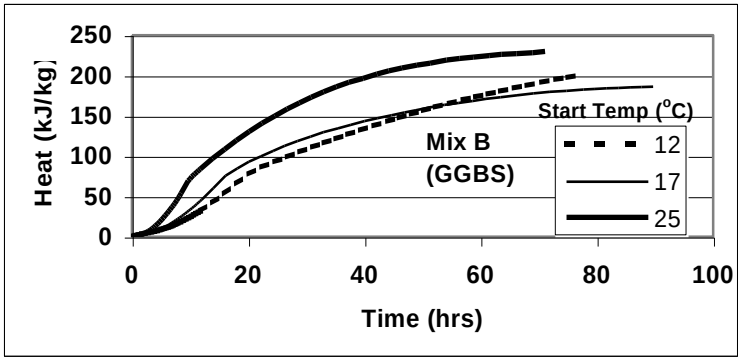

(b)

Fig. 2. Calculated heat output for the three adiabatic tests conducted on each concrete mixture

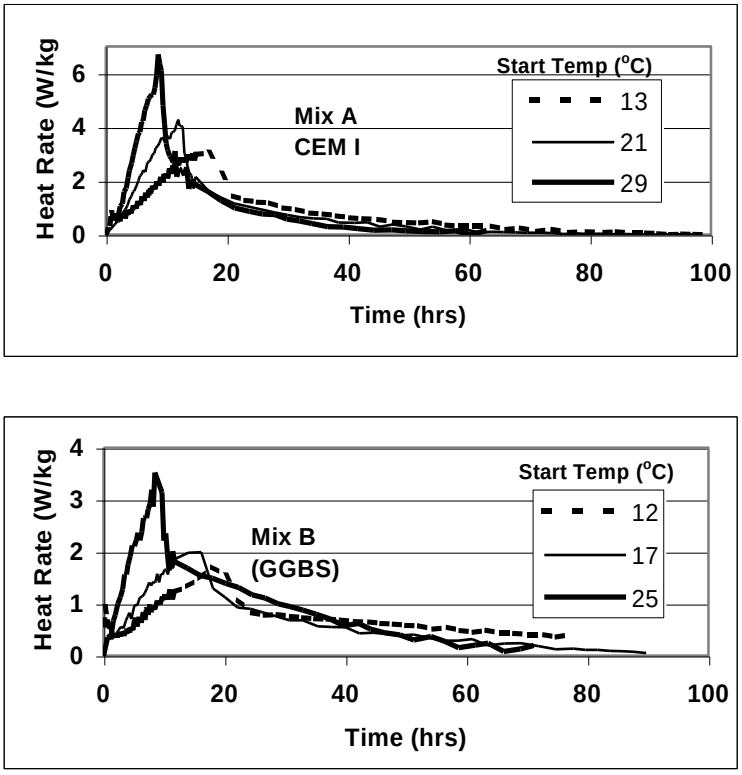

(a)

(b)

Fig. 3. Variation of the time-based heat rates determined from the adiabatic tests

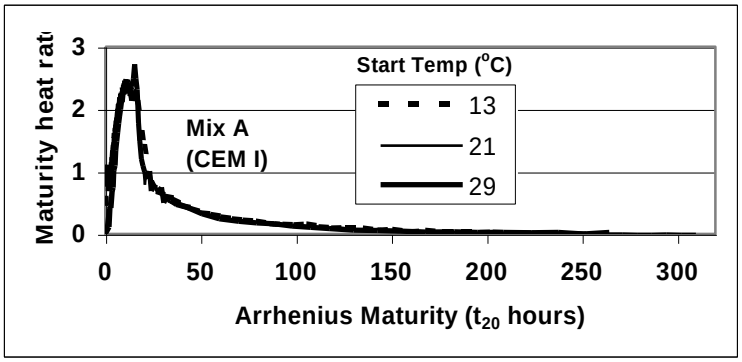

(a)

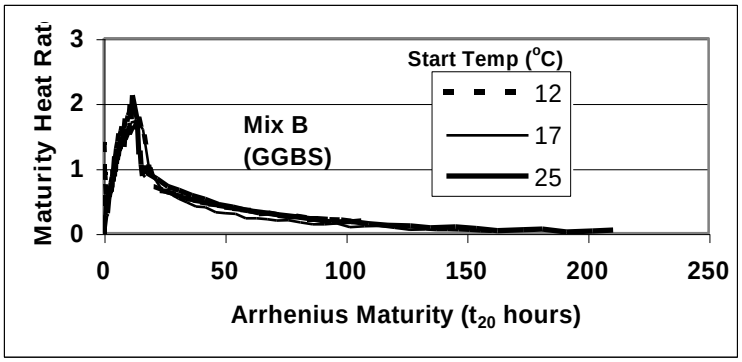

(b)

Fig. 4. Heat rates expressed in terms of maturity using the Arrhenius maturity function for the two concretes assessed.

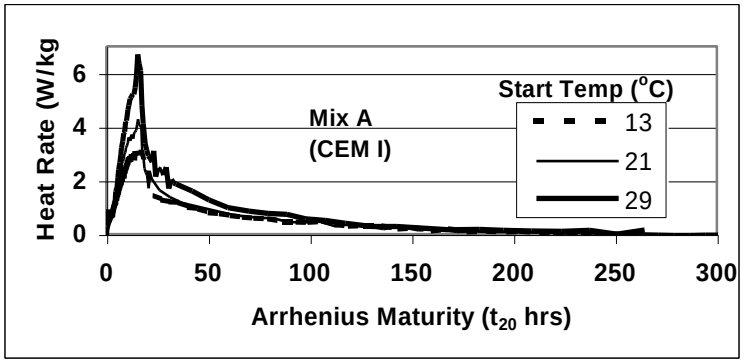

Figure 5: Heat rates of the CEM I concrete expressed in terms of maturity using the Nurse-Saul maturity function

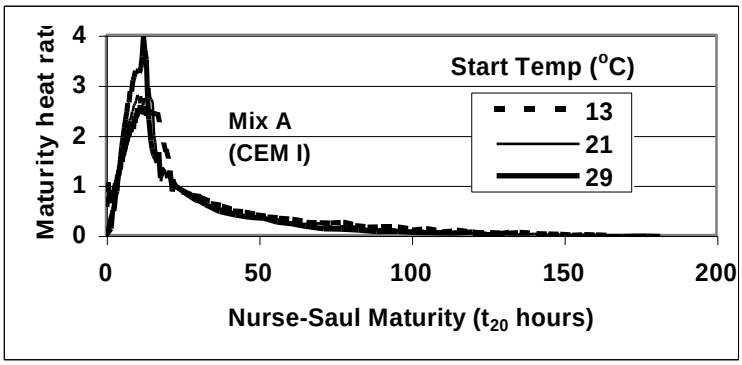

Figure 6: Relationship between the time-based heat rate ($\dot{q}_t$) of the CEM I concrete samples and the corresponding Arrhenius maturity.

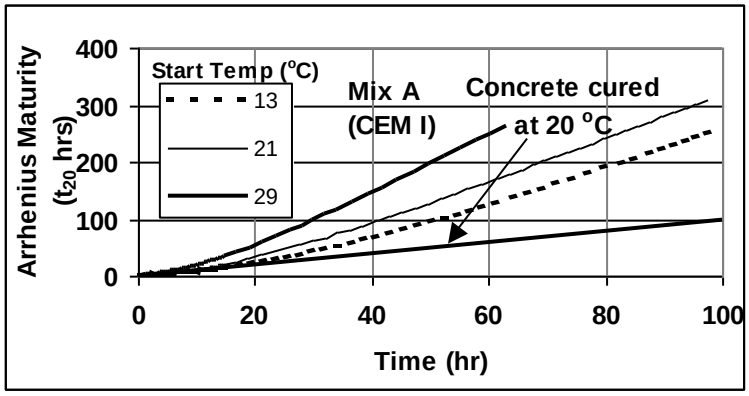

Fig. 7. Variation in cumulative maturity of the CEM I concrete in the three adiabatic tests